© Strojniški vestnik 49(2003)10,484-498
ISSN 0039-2480
UDK 621.224.24:532.528
Izvirni znanstveni članek (1.01)

© Journal of Mechanical Engineering 49(2003)10,484-498
ISSN 0039-2480
UDC 621.224.24:532.528
Original scientific paper (1.01)

Vpliv tlačnih utripanj v sesalni cevi na dinamiko kavitacijskega vrtinca v francisovi turbini

The Influence of Draft-Tube Pressure Pulsations on the Cavitation-Vortex Dynamics in a Francis Turbine

Marko Hočevar - Brane Širok - Igor Grabec - Tomaž Rus

V prispevku je predstavljen vpliv tlačnih utripanj na dinamiko kavitacijskega vrtinca v sesalni cevi francisove turbine. Pri eksperimentalnem delu na modelu francisove turbine so bila hkrati merjena utripanja tlaka na steni sesalne cevi in dinamika kavitacijskega vrtinca. Dinamika kavitacijskega vrtinca je bila merjena z metodo vizualizacije.

Predstavljena je metoda, s katero je mogoče napovedati dinamiko kavitacijskega vrtinca na podlagi izmerjenih tlačnih utripanj v eni točki na steni sesalne cevi. Uspešnost napovedi je bila v povprečju zelo dobra. Napoved dinamike kavitacijskega vrtinca je bila uspešnejša v primerih, ko je bil kavitacijski vrtinec v bližini tlačnega zaznavala.

(Ključne besede: turbine francis, vrtinci kavitacijski, utripanja tlačna, vizualizacija)

The influence of pressure pulsations on the cavitation-vortex dynamics in a Francis-turbine draft tube is presented. The experiment was performed on a model Francis turbine in which pressure pulsations on the draft-tube wall and the cavitation-vortex dynamics were acquired simultaneously. The cavitation-vortex dynamics was recorded using a visualization method.

An experimental model was proposed in which the cavitation-vortex dynamics was predicted based on recorded pressure information at one point on the draft-tube wall. The performance of the model is, on average, very good. The prediction of the cavitation-vortex dynamics shows better results when the distance between the pressure sensor and the cavitation vortex is short.

(Keywords: Francis turbines, vortex cavitation, pressure pulsation, visualization)

0 UVOD

Podobnost med strukturo kavitacijskega vrtinca in tlačnimi utripanji je poznana. Kljub temu je informacij o funkcijski povezanosti med strukturo vrtinca in tlačnimi utripanji malo. Naš namen je napovedati povprečno svetlost in strukturo kavitacijskega vrtinca, če poznamo tlak na steni sesalne cevi francisove turbine.

Kavitacijski vrtinec v hidravličnih strojih spreminja hidrodinamiko toka, povečuje hidrodinamični upor in povzroča nihanja, še posebej pri obratovanju z delno obremenitvijo. Z vidika izdelovalcev in uporabnikov turbine je zato ugodno, če poznamo kavitacijski vrtinec v sesalni cevi turbine. V tej raziskavi želimo podati

0 INTRODUCTION

The similarity between the structure of a cavitation vortex and the pressure pulsations in a draft tube is known, but there is a lack of information about functional relations between the vortex structure and the pressure pulsations. Our goal was to predict the average image intensity and the cavitation-vortex structure, provided that the pressure in the draft-tube wall of a Francis turbine is known.

The cavitation vortex in hydraulic machines generates vibrations, increases hydrodynamic drag, changes flow hydrodynamics, especially during part-load operation. From the turbine designer's and the operator's points of view, it is therefore desirable to know whether and to what extent the cavitation vortex

mogočo rešitev tega problema. Model, ki je predstavljen v tem prispevku, omogoča napovedovanje strukture kavitacijskega vrtinca v primeru, da poznamo dinamiko spreminjanja tlaka na steni sesalne cevi. Tako oblikovan model se bo lahko uporabljal za prepoznavanje kavitacijskih režimov v sesalnih ceveh vodnih turbin in njihovo prilagodljivo krmiljenje.

Napovedovanje dinamike kavitacijskega vrtinca je problem, ki ga je obravnavalo več avtorjev ([1] do [5]). Za opis pojava so bili uporabljeni numerični ([6] in [7]) ter analitični modeli ([1], [2] in [8]).

V tem prispevku smo uporabili metodo napovedi, ki je podobna razpoznavanju vzorcev razumnih bitij in temelji na statističnem modeliranju. Metoda temelji na informacijah, dobljenih s predhodnimi opazovanji istega pojava v ustreznem okolju. Informacije so predstavljene kot podatki o tlaku in strukturi kavitacijskega vrtinca. Izmerjeni in zapisani podatki so temelj za osnovne parametre statističnega modela. Tak model ima strukturo nevronske mreže (NM) [9].

Nevronska mreža deluje na dva različna načina, ki ju imenujemo učenje in napoved. Med učenjem nevronska mreža dobi eksperimentalne podatke o vhodnih in izhodnih intervalih, ki sta lahko ločena v času in prostoru. Ti skupni podatki so shranjeni v spominu nevronske mreže in tvorijo eksperimentalno osnovo modela. Med napovedjo dobi nevronska mreža samo del podatkov v vhodnem intervalu in napove podatke v izhodnem intervalu. Ker kavitacijski vrtinec v splošnem opazujemo prek meritev tlačnih utripanj na steni sesalne cevi ([1] in [2]), smo te podatke uporabili kot vhodni interval za nevronsko mrežo. Za krmiljenje toka nevronske mreže ponujajo možnost prilagodljivega krmiljenja, ki je preprostejši in pogojno manj občutljiv na variacije parametrov kakor običajni krmilniki [10].

V nadaljevanju prispevka bomo predstavili eksperimentalni del in metodo napovedi. Delovanje metode napovedi bomo ocenjevali s primerjavo lastnosti izmerjene in napovedane povprečne svetlosti slike kavitacijskega vrtinca in celotnih slik kavitacijskega vrtinca. Povprečne svetlosti slik uporabljamo kot merilo za delež plinske faze kavitacijskega vrtinca, celotne slike pa kot merilo za strukturo kavitacijskega vrtinca. V nadaljevanju bomo opisali povezavo med tlačnimi utripanji na steni sesalne cevi in strukturo vrtinca. Povezava bo temeljila na obliki in utripanjih tlačnega signala. Rezultate bomo primerjali z objavljenimi rezultati parametričnega modela [11] napovedi kavitacijskega vrtinca.

is present in the draft tube of a turbine. In our investigation we wanted to provide a possible solution to this problem. The model presented here allows us to predict the cavitation vortex structure by knowing only the pressure in the draft tube. In future this could be useful in cases where the draft tube in not accessible, for example, in real power plants. A model designed in this way could be used for the detection of cavitation regimes and for adaptive control.

The prediction of cavitation-vortex dynamics is a problem that has been treated by many authors ([1] to [5]). Several numerical ([6] and [7]), or analytical ([1], [2] and [8]) models can be used to describe the phenomena and the behavior of a cavitation vortex.

We used a prediction method that is similar to the recognition of patterns by intelligent beings and based on statistical modeling. The method uses the information provided by previous observations of the same phenomenon in an equivalent environment. The information is presented as joint data about the pressure and the structure of the cavitation vortex. The recorded and stored data provide the basic parameters of the statistical model. It appears that such a model exhibits a structure of artificial neural networks (ANN) [9].

The ANN operates in two different modes: learning and prediction. During learning, the ANN obtains experimental data from the input and output intervals that can be separated in time and space. These joint data are stored in the memory of the ANN and form the experimental basis of the model. During prediction, the ANN obtains only partial data from the input interval, and predicts the data in the output interval. Since the cavitation vortex is generally observed indirectly through pressure-pulsation measurements on the draft-tube wall ([1] and [2]), we use these data as an input interval for the ANN. For flow-control applications, the ANN offers the possibility of adaptive controllers, which are simpler and potentially less sensitive to parameter variations than conventional controllers [10].

In the following sections of the paper we present the experimental arrangement and the prediction method. Then, we estimate the performance of the method by comparing the properties of the predicted and the corresponding measured average cavitation-vortex image intensities, and the entire images of the cavitation vortex. The average image intensities are used as a measure of the cavitation-vortex void fraction, while the entire images are used as a measure of the cavitation-vortex structure. The results of the prediction will be presented for several operation points. The interdependence between the pressure in the draft-tube wall and the structure of the vortex will be discussed, based on the overall structure and fluctuations of the pressure signal. The results will be compared with previously published results [11] of predicting the parametric cavitation vortex.

1 POSKUS

Poskusno delo je potekalo na modelu francisove turbine. Shema poskusa je predstavljena na sliki 1. Delovne razmere modelne turbine smo določili s spreminjanjem odprtja, vrtilne frekvence in tlaka. Izbrali smo dvajset delovnih točk z različnimi pretočnimi števili, tlačnimi števili in kavitacijskimi števili.

Meritve tlačnih utripanj smo izvedli s piezoelektričnim tlačnim pretvornikom Kistler, ki je bil nameščen na steni sesalne cevi turbine in povezan z notranjostjo z izvrtino premera 4 mm. Meritve tlačnih utripanj smo posneli s 16-bitno merilno kartico National Instruments s frekvenco vzorčenja 15 kHz. Signal smo filtrirali z eliptičnim filtrom 8. reda in frekvenco 5 kHz.

Slike kavitacijskega vrtinca smo posneli s sistemom za hitro vzorčenje slik, ki je bil sestavljen iz kamere CCD DALSA CA D-1/256 in kartice za zajemanje slik IC PCI z modulom AM DIG. Ločljivost kamere je znašala 256×256 točk. Frekvenca vzorčenja je znašala 175 Hz. Skupno smo v vsaki delovni točki posneli 4400 slik. Za osvetlitev kavitacijskega vrtinca smo uporabili monokromatsko svetlobo, ki je vstopala v sesalno cev skozi okno iz poliakrilnega stekla.

Vzorčenje signala tlaka in slik smo sinhronizirali s prožilnim signalom iz merilne kartice za vzorčenje tlaka. Osi zaznavala tlaka in kamere CCD sta bili nameščeni v isti vodoravni ravnini pod kotom 90°.

1 THE EXPERIMENT

The experimental work was performed on a model Francis-turbine test rig. The layout of the experiment is presented in Fig. 1. The operating conditions of the turbine model were set during the experiment by varying the opening, the rotation speed of the model and the pressure in the system. Twenty operation points with different flow coefficients, pressure coefficients, and cavitation numbers were selected.

The pressure was measured with a Kistler piezoelectric pressure transducer, mounted directly into the wall of the turbine draft tube and connected to the turbine flow tract through a 4-mm-diameter hole. The measured pressure signals were then transferred to a processing computer with an installed 16-bit A/D data-acquisition board from National Instruments. The bandwidth of the pressure adapter was 5 kHz, and the sampling frequency was 15 kHz (via an 8-pole elliptic filter).

Images of the cavitation vortex were acquired using a fast digital-video system composed of a CCD camera, DALSA CA D-1/256, and an IC PCI image-acquisition board with an AM DIG module. The resolution of the camera was 256×256 pixels. The frequency of the image acquisition was 175 Hz, and the camera's exposure time was 0.005 s. A total of 4400 images were recorded for each operation point. The monochrome light entering the draft tube through a Plexiglas window provided the illumination for the cavitation vortex in the draft tube.

The sampling of the pressure and video signal was synchronized with the triggering signal from the data-acquisition board used to acquire the pressure. The axes of the pressure sensor and of the CCD camera were located in the same horizontal plane at an angle of 90°.

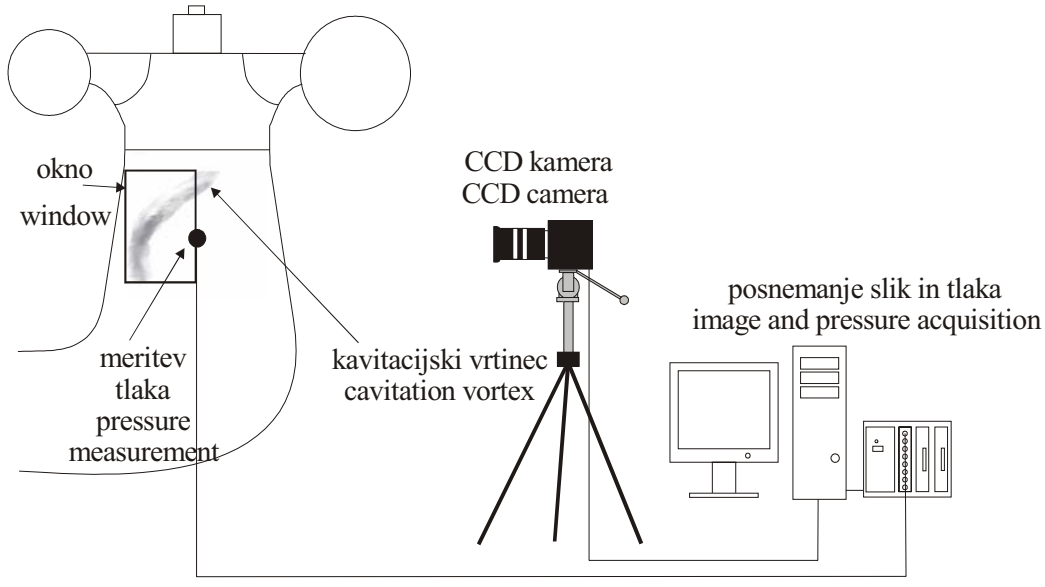

Sl. 1. *Shema poskusa*
Fig. 1. *The experimental set-up*

1.1 Predobdelava slik

Za doseganje dobre kakovosti posnetih slik je treba zagotoviti ustrezno namestitev kamere in sistema za osvetljevanje. To je bilo v primeru modelne francisove turbine oteženo zaradi omejenega prostora za namestitev kamere in svetilnih teles. S predhodno obdelavo slik smo zmanjšali odboje, vpliv ozadja in šuma ter izboljšali kontrast.

1.2 Povprečna svetlost slike v izbranem oknu

Povprečno svetlost slike v izbranem oknu smo izračunali iz slik po predhodni obdelavi. Izbrali smo okno velikosti 300 x 150 mm, ki je pokrivalo polovico poldnevne ravnine sesalne cevi pod rotorjem turbine, kar prikazuje slika 1. Izbrali smo okno enake velikosti kakor v [11]. Če predpostavimo, da je kinematika kavitacijskega vrtinca simetrična glede na os turbine, smo tako dosegli največji odziv optičnega signala na vrtilno gibanje kavitacijskega vrtinca v sesalni cevi. Za kvantitativno določitev obnašanja kavitacijskega vrtinca smo uvedli skalarno spremenljivko *A(t)* [12]:

Spremenljivka *A(t)* označuje povprečno svetlost v opazovanem oknu na sliki, posneti ob času *t*. *E* je svetlost točk s koordinato (*l,m*) v oknu. Ker smo uporabili 8-bitno monokromatsko kamero, so bile vrednosti spremenljivke *E* v območju od 0 do 255.

1.3 Stiskanje slike z diskretno valčno transformacijo (DVT)

Za nadaljnje napovedovanje celotne strukture slik kavitacijskega vrtinca z nevronskimi mrežami je bilo potrebno zaradi zmanjšanja računske obremenitve ločljivost obstoječe slike velikosti 256 x 256 točk zmanjšati. Izmed različnih možnih algoritmov smo izbrali DVT [13]. DVT ponuja prikaz slike na več nivojih ločljivosti, pri tem pa daje dobro učinkovitost stiskanja ([14] in [15]). Zaradi navedenih prednosti je stiskanje slik z DVT zelo uporabno orodje za različne znanstvene uporabe [16].

Primer uporabe algoritma DVT je prikazan na sliki 2. Ločljivost slike je bila zmanjšana iz 256 x 256 točk na 36 x 36 točk. S slike je razvidno, da se osnovne značilnosti strukture vrtinca ohranjajo, kar potrjuje uporabnost metode.

1.1 Image pre-processing

To achieve good-quality images, proper positioning of both the camera and the illumination system is required. This is usually limited by the space around the test rig. In our case, images were pre-processed in order to eliminate reflection, background and noise, and to improve the contrast.

1.2 Average image intensity of the selected window

The average image intensity of a selected window was calculated from the filtered images. A window of 300 by 150 mm was selected, which covered half of the meridian plane of the draft tube, directly beneath the turbine rotor, as shown in Figure 1. To make possible a comparison of the results, the same size of window was used as in [11]. Assuming that the cavitation vortex kinematics was axisymmetrical, the maximum response of the optical signal on the rotational vortex movement in the draft tube was obtained. For the assessment of the quantitative behavior of the patterns within the cavitation vortex, the following integer-type scalar variable *A(t)* was introduced [12] :

$$A(t) = \sum_{l=1}^{300} \sum_{m=1}^{150} E(l,m) \qquad (1).$$

The variable *A(t)* denotes the average intensity in the observed window in the image recorded at time *t*. Here, *E* is the intensity of pixels with spatial coordinates (*l,m*) inside the window. We used an 8-bit monochromatic camera, thus the values of *E* were in the range from 0 to 255.

1.3 Image compression using the Discrete Wavelet Transformation (DWT) algorithm

For further prediction of the entire cavitation images using neural networks, the existing image size of 256x256 pixels had to be reduced to lower the computational burden. From among various, available image-compression algorithms we chose the DWT, which has recently become popular for image-coding applications. The DWT inherently provides a multi-resolution image representation, while also improving the compression efficiency ([14] and [15]). These benefits make image compression using the DWT a very useful tool for various scientific applications [16].

A sample image showing the efficiency of the applied DWT is shown in Fig. 2. The resolution of the image was reduced from 256x256 pixels to 36x36 pixels. Figure 2 shows that the basic properties of the image are preserved, so confirming the suitability of the method.

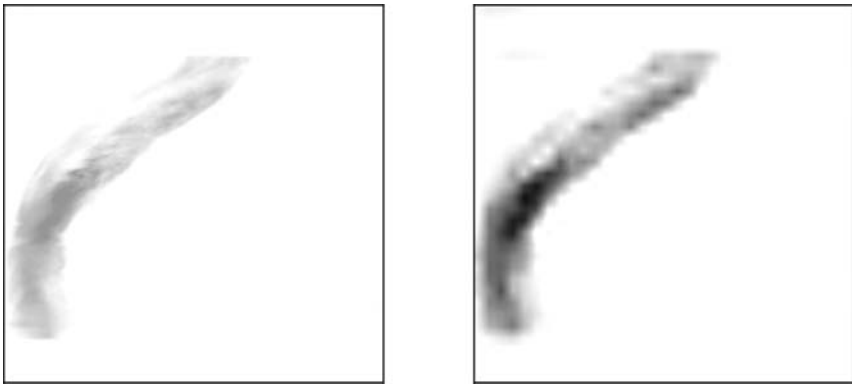

Sl. 2. *Primer slike (levo) brez stiskanja, ista slika (desno) po predobdelavi in stiskanju z DVT*
Fig. 2. *Sample image (left) without compression, the same image after pre-processing and DWT compression (right).*

2 EKSPERIMENTALNO NAPOVEDOVANJE KAVITACIJSKEGA VRTINCA Z RADIALNIMI BAZNIMI NEVRONSKIMI MREŽAMI (RBNM)

Naravne zakone običajno opišemo kot zvezo med odvisnimi in neodvisnimi spremenljivkami $\mathbf{y} = f(\mathbf{x})$. V našem primeru $\mathbf{x}$ pomeni neodvisni oziroma dani vektor (tlačno utripanje), medtem ko $\mathbf{y}$ pomeni odvisne podatke (povprečno svetlost slike oziroma slike kavitacijskega vrtinca). Osnovni problem ob tem je določiti metodo, s katero je mogoče določiti funkcijo f na podlagi danih skupnih eksperimentalnih podatkov. V ta namen smo uporabili neparametričen postopek z RBNM.

Diagram RBNM je prikazan na sliki 3. RBNM je sistem za obdelavo podatkov, sestavlja ga K spominskih celic, ki se imenujejo nevroni in imajo lokalno polje sprejemanja. To polje opisuje radialna simetrična bazna funkcija $g(\mathbf{x})$ vhodnega vektorja $\mathbf{x}$. Uporabili smo Gaussovo funkcijo $g_k(\mathbf{x})$ [9]:

2 EXPERIMENTAL PREDICTION OF THE CAVITATION VORTEX USING RADIAL BASIS NEURAL NETWORKS (RBNN)

A natural law is usually described as a relationship between dependent and independent variables $\mathbf{y} = f(\mathbf{x})$. In our case, $\mathbf{x}$ represents the independent or given data vector (pressure pulsations), while $\mathbf{y}$ describes the dependent data (average window intensity or cavitation-vortex images). The fundamental problem is to formulate a method by which a function f can be predicted on the basis of the joint experimental data. A non-parametric approach using RBNN was applied for this purpose.

A diagram of RBNN is shown in Fig. 3. RBNN is an information-processing system consisting of K memory cells, called neurons, with a localized receptive field. This field is described by a radially symmetrical basis function $g(\mathbf{x})$ of the input vector $\mathbf{x}$. We employed the Gaussian function, $g_k(\mathbf{x})$ [9]:

$$g_k(\mathbf{x}) = \exp\left(-\frac{\|\mathbf{x}-\mathbf{q}_k\|^2}{2\sigma_k^2}\right) \quad (2),$$

v kateri parametri $\mathbf{q}_k$ in σ_k označujejo središča in širino polja sprejemanja k-tega nevrona. Vsi nevroni

in which the parameters $\mathbf{q}_k$ and σ_k denote the center and the width of the receptive field of the k-th

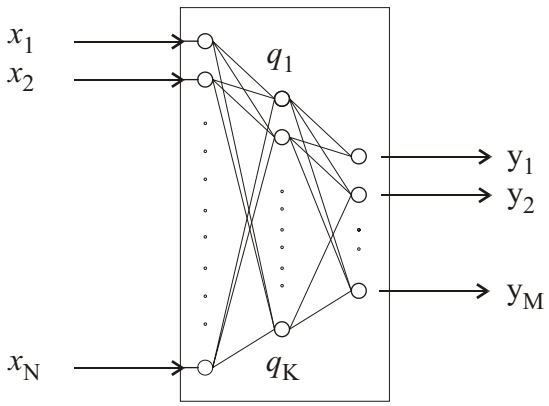

Sl. 3. *Shema RBNM*
Fig. 3. *Diagram of the RBNN*

dobijo enak vhod **x**. Izhod $y(\mathbf{x})$ nevronske mreže je superpozicija posameznih izhodov:

$$\mathbf{y}(\mathbf{x}) = \sum_{k}^{K} m_k g_k(\mathbf{x}) \tag{3}.$$

Ta superpozicija pomeni model funkcije *f,* ki jo določa množica parametrov m_k, $\mathbf{q}_k$ in σ_k. Parametre statistično ocenimo iz dane množice eksperimentalnih vzorcev ($\mathbf{x}_n$, $\mathbf{y}_n$), $n = 1 \ldots N$, tako da je povprečno kvadratično neujemanje med izhodom $\mathbf{y}(\mathbf{x}_n)$ in eksperimentalnim podatkom $\mathbf{y}_n$ najmanjše:

$$E\left[\left(\mathbf{y}(\mathbf{x}_n) - \mathbf{y}_n\right)^2\right] \Rightarrow \min(m_k, \sigma_k, q_k) \tag{4}.$$

Na voljo so številni algoritmi za zmanjšanje te kriterijske funkcije; uporabili smo algoritem, ki temelji na programskem paketu Matlab.

Pri napovedovanju smo kot vhodni vektor stanja **x** uporabili tlak na steni sesalne cevi. Izhod **y** predstavlja ustrezno strukturo kavitacijskega vrtinca, ki je lahko povprečna svetlost slike ali celotna slika.

Dolžina učne množice je bila omejena na 4000 vhodno-izhodnih dvojic (**x**, **y**). Obnašanje modela smo preskusili na testni množici, ki je vsebovala 400 dvojic. Število nevronov *K* je bilo 2000, kar pomeni polovico števila dvojic (**x**, **y**), ki so bili uporabljeni za učenje.

Dolžino *j* časovno zakasnjenega vhodnega vektorja **x**, oziroma potek tlačnih utripanj, smo uvedli v nevronsko mrežo z zvezo:

$$\mathbf{x} = \left(p(t),\ p(t - \frac{1}{f_p}),\ p(t - 2 \cdot \frac{1}{f_p}),\ \ldots\ , p(t - j \cdot \frac{1}{f_p}) \right) \tag{5},$$

f_p je frekvenca vzorčenja tlaka *p*. Dolžina *j* časovno zakasnjenega vektorja je bila 20 vzorcev. Izbrana vrednost je omogočala najboljšo povprečno kakovost napovedi in je ustrezala približno polovici osnovne periode gibanja kavitacijskega vrtinca. Frekvenca vzorčenja tlaka f_p je bila zmanjšana na 175 Hz, kar je bilo enako frekvenci vzorčenja slik. Enake vrednosti za *j* in f_p smo uporabljali v vseh delovnih točkah.

3 REZULTATI IN RAZPRAVA

Vsaka delovna točka turbine vsebuje značilno dinamiko kavitacijskega vrtinca, kar vpliva na rezultate napovedovanja. Kakovost napovedovanja smo ocenjevali z regresijskimi koeficienti r_w in povprečnimi regresijskimi koeficienti $\bar{r}_i$. Poenostavitvene koeficiente r_w smo izračunali iz 400 zaporednih povprečnih svetlosti slik

neuron, respectively. All neurons have the same input **x**. The output **y**(**x**) from the network is described by a linear superposition of the individual outputs:

This superposition represents the model of function *f*, which is specified by the set of parameters, m_k, $\mathbf{q}_k$ and σ_k. These parameters are statistically estimated from a given set of experimental samples ($\mathbf{x}_n$,$\mathbf{y}_n$), $n = 1 \ldots N$, so that the mean-square error between the network output $\mathbf{y}(\mathbf{x}_n)$ and the experimental datum $\mathbf{y}_n$ is minimized:

Various algorithms for minimizing this criterion function are available; we used the algorithm based on the Matlab software package.

In our prediction, the pressure in the draft-tube wall was used as the input **x**. The output **y** denotes the corresponding cavitation-vortex structure, which was either an average image intensity or an entire image.

The length of the learning set in this study was limited to 4000 (**x**, **y**) input-output pairs. The behavior of the model was tested on a prediction set that included 400 sample pairs. The number of neurons, *K,* was set to 2000, half of the number of (**x**, **y)** sample pairs used for the training.

Using length *j* of the time-delayed input vector **x**, the history of pressure pulsations was introduced into the network

here f_p is the frequency of the acquired pressure, *p*. The length, *j*, of the time-delayed input vector **x** was set to 20 samples. This value was found to provide the best average-prediction performance, and to correspond to roughly half the basic period of the cavitation-core movement. The frequency of the pressure input, f_p, was downsampled to 175 Hz, which was the same as the frequency of the image acquisition. Once the values of *j* and f_p were set, they were used for all operation points.

3 RESULTS AND DISCUSSION

Each operating point of the turbine posesses a characteristic dynamics of the cavitation-vortex behavior, which affects the prediction performance. The prediction performance was estimated by the regression coefficients, r_w, and the average regression coefficients, $\bar{r}_i$. The regression coefficients, r_w, were calculated from 400 successive, predicted average

kavitacijskega vrtinca. Poenostavitveni koeficienti r_w so primerljivi z rezultati iz [11]. Povprečni regresijski koeficienti $\bar{r}_i$ so povprečje prek 400 zaporednih regresijskih koeficientov r_i. Poenostavitveni koeficienti r_i so dvorazsežni regresijski koeficienti med izmerjenimi in napovedanimi slikami. Poenostavitveni koeficienti r_w in $\bar{r}_i$ so prikazani v preglednici 1.

Regresijski koeficienti r_w povprečne svetlosti slike so v območju od 0,82 do 0,99, regresijski koeficienti $\bar{r}_i$ celotne slike pa so v območju od 0,59 do 0,88. Visoke vrednosti regresijskih koeficientov r_w in $\bar{r}_i$ kažejo dobro napoved uporabljene metode. Iz preglednice 1 je tudi razvidno, da velja $\bar{r}_i < r_w$ za vse delovne točke. Razlog za to vidimo v visokorazseži strukturi kavitacijskega vrtinca, ki jo napovedujemo z nižjerazsežnim signalom tlaka, merjenim zgolj v eni točki na steni sesalne cevi. Čeprav je meritev v eni točki ugodna z vidika preproste uporabe modela in morebitne uporabe v krmilne namene, lahko predpostavljamo, da je za doseganje boljših rezultatov treba zagotoviti drobnejši opis strukture kavitacijskega vrtinca. Primerjava z rezultati v [11] je prikazana na sliki 4. V obeh primerih je bila uporabljena ista modelna turbina in iste delovne točke, zato je med rezultati mogoča neposredna primerjava. Rezultati modela, predstavljenega v tem prispevku, so boljši od rezultatov, predstavljenih v [11]. S slike 4 je tudi razvidno, da imajo delovne točke z visokim regresijskim koeficientom $\bar{r}_i$ tudi visok regresijski koeficient r_w in nasprotno. Značilna razlika med rezultati, predstavljenimi v tem prispevku, in rezultati [11] je, da so bili v delu [11] uporabljeni isti podatki za učno in testno množico, v tem prispevku pa sta bili testna in učna množica ločeni.

Poleg uspešnosti z regresijskimi koeficienti bomo ocenjevali še uspešnost napovedovanja s primerjavo časovnih vrst izmerjenih in napovedanih podatkov. To bo opisano v naslednjih dveh podpoglavjih.

intensities of the cavitation-vortex images, and are comparable with the results in [11]. The average regression coefficients, $\bar{r}_i$, were averaged over 400 successive regression coefficients, r_i. The regression coefficients, r_i, are two-dimensional regression coefficients between the measured and the predicted images. The regression coefficients r_w and $\bar{r}_i$ are shown in Table 1.

The regression coefficients, r_w, of average window-intensity prediction are in the range from 0.82 to 0.99, and the regression coefficients, $\bar{r}_i$, of the entire image prediction are in the range from 0.59 to 0.88. The high values of the regression coefficients, r_w and $\bar{r}_i$, show the good prediction performance of the method. Table 1 also shows that $\bar{r}_i < r_w$ for all the operation points. The reason for this is that the high-dimensional cavitation-vortex structure is predicted by providing a lower-dimensional pressure only, and measured at only one location in the draft-tube wall. While the measurement at one point is highly desirable in terms of the model's ease of use and possible control, it can be surmised that a finer-detail description of the vortex structure would be necessary to achieve better performance. A comparison with the results in [11] is shown in Fig. 4. The same turbine and the same operation points were selected in both cases, so that a direct comparison between the two models is possible. On average, the performance of the model presented here is better than that of the model presented in [11]. Fig. 4 also shows that the operation points with high $\bar{r}_i$ have, on average, high r_w, and vice versa. A notable difference between this work and the work performed in [11] is that in [11], the same set of data was used for the learning and the prediction, which was not the case here.

As well as using regression coefficients, we estimated the prediction performance by comparing time series of the measured and predicted data. This will be described in the next two subsections.

Preglednica 1. *Regresijski koeficienti za napovedovanje povprečne svetlosti slike (r_w) in napovedovanje celotnih slik ($\bar{r}_i$) kavitacijskega vrtinca*
Table 1. *Regression coefficients for the average image prediction (r_w) and the entire cavitation-vortex image prediction ($\bar{r}_i$)*

delovna točka operation point	r_w	$\bar{r}_i$	delovna točka operation point	r_w	$\bar{r}_i$
1	0,90	0,76	11	0,93	0,68
2	0,91	0,75	12	0,99	0,88
3	0,97	0,70	13	0,95	0,81
4	0,95	0,79	14	0,89	0,62
5	0,97	0,79	15	0,94	0,78
6	0,88	0,62	16	0,86	0,61
7	0,92	0,66	17	0,88	0,63
8	0,82	0,61	18	0,95	0,76
9	0,96	0,85	19	0,82	0,59

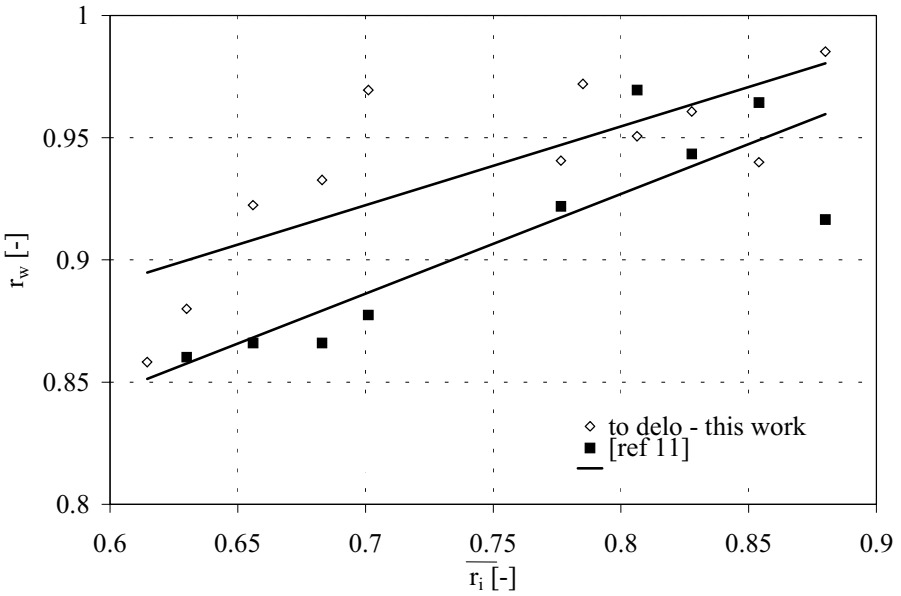

Sl. 4. *Odvisnost regresijskih koeficientov povprečne svetlosti slike r_w od povprečnih regresijskih koeficientov napovedi celotnih slik $\overline{r_i}$. Eksperiment je bil izveden na isti modelni turbini in v istih delovnih točkah kakor v [11].*

Fig. 4. *Dependence of the regression coefficients for the average image-intensity prediction, r_w, on the regression coefficients for the entire image prediction, $\overline{r_i}$. The experiment in this study and in [11] were performed using the same rotor and the same operation points.*

3.1 Napovedovanje povprečne svetlosti slike

V tem podpoglavju bomo podrobneje ocenjevali napovedovanje povprečne svetlosti slike v delovnih točkah 12, 6 in 8.

Kakovost napovedovanja za delovno točko 12 je prikazana na sliki 5 (r_w = 0,99). Najpomembnejša ugotovitev je dobro ujemanje med napovedanimi in izmerjenimi povprečnimi svetlostmi slike. Izmerjena in napovedana povprečna svetlost slik sta razmeroma gladki in navidezperiodični. Podobno gladko obnašanje opazimo pri tlačnih utripanjih na steni sesalne cevi, toda tlačni signali so fazno zakasnjeni v primerjavi s signalom povprečne svetlosti slike. Slika 5 kaže, da v primeru, ko je kavitacijski vrtinec blizu tlačnega zaznavala, ta zazna tlačni minimum in nasprotno. Fazni odmik med tlačnim signalom in povprečno svetlostjo slike je rezultat odmika zaradi postavitve zaznaval in izbire delovne točke [11]. Model pravilno napove fazo. Zaradi dobrega ujemanja med izmerjeno in napovedano povprečno svetlostjo slike predpostavljamo, da je obnašanje kavitacijskega vrtinca v tej delovni točki navidezdeterministično.

Napovedovanje v delovni točki 6 je predstavljeno na sliki 6 (r_w = 0,88). Ugotovili smo, da je kakovostno ujemanje med izmerjenimi in napovedanimi povprečnimi svetlostmi slik dobro celo v nekaterih visokofrekvenčnih podrobnostih. Kljub razmeroma pravilnemu gibanju

3.1 Average image-intensity prediction

In the following subsection, the performance of the average image-intensity prediction at three operation points, 12, 6 and 8, will be discussed in more detail.

The prediction performance for operation point 12 is shown in Fig. 5 (r_w = 0.99). The most outstanding feature here is the good agreement between the predicted average image intensities and the measured average image intensities. Both the experimental and the predicted average image intensities are relatively smooth and quasi-periodic. The same smooth behavior is observed with pressure fluctuations in the draft-tube wall, but the pressure fluctuations are phase-shifted when compared to the average image intensity. Fig. 5 shows that when the vortex is near the pressure sensor, the sensor senses a pressure minimum, and vice versa. The phase shift between the pressure signal and the average image intensity is the result of a shift due to the placement of sensors, and of the selection of the operation point [11]. The model is able to reproduce the phase correctly. From the good agreement between the experimental and predicted average image intensities we assume that the cavitation-vortex behavior at this operating point has a quasi-deterministic nature.

The prediction performance for operation point 6 is shown in Figure 6 (r_w = 0.88). We observed that the qualitative agreement between the measured and predicted average image intensities is good, even in some of the higher-frequency details. In spite of the relatively regular motion of the cavitation

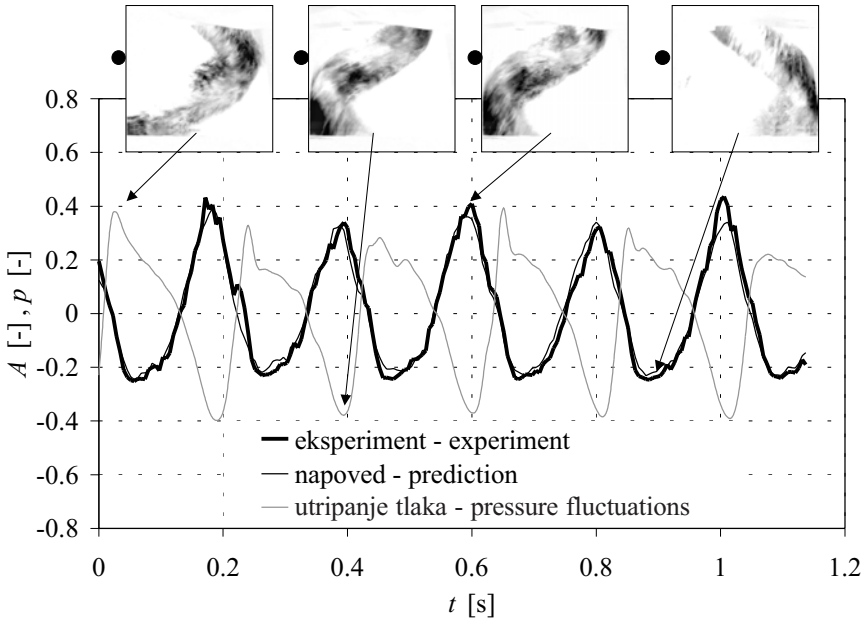

Sl. 5. *Napoved povprečne svetlosti slike, delovna točka 12 (r_w = 0,99). Lega tlačnega zaznavala je prikazana s točko ob posamezni sliki kavitacijskega vrtinca.*
Fig. 5. *Prediction of the average window-intensity operation point 12 (r_w = 0.99). The location of the pressure sensor is shown by a dot beside each representative image.*

kavitacijskega vrtinca (sl. 9, levo), lahko opazimo utripno obnašanje povprečne svetlosti slike in tlaka na steni sesalne cevi. Močna tlačna utripanja na steni sesalne cevi kažejo na nestabilno naravo kavitacijskega vrtinca v tej delovni točki. Utripanja so odvisna od povprečne debeline kavitacijskega vrtinca oziroma deleža plinske faze (sl. 9).

vortex (Fig. 9, left), the fluctuating behavior of the average image intensities and the pressure in the draft-tube wall can be seen. Strong pressure pulsations in the draft-tube wall indicate the unstable nature of the cavitation vortex for this operation point. These pulsations are dependent on the average vortex thickness and the cavitation-vortex void fraction (Fig. 9).

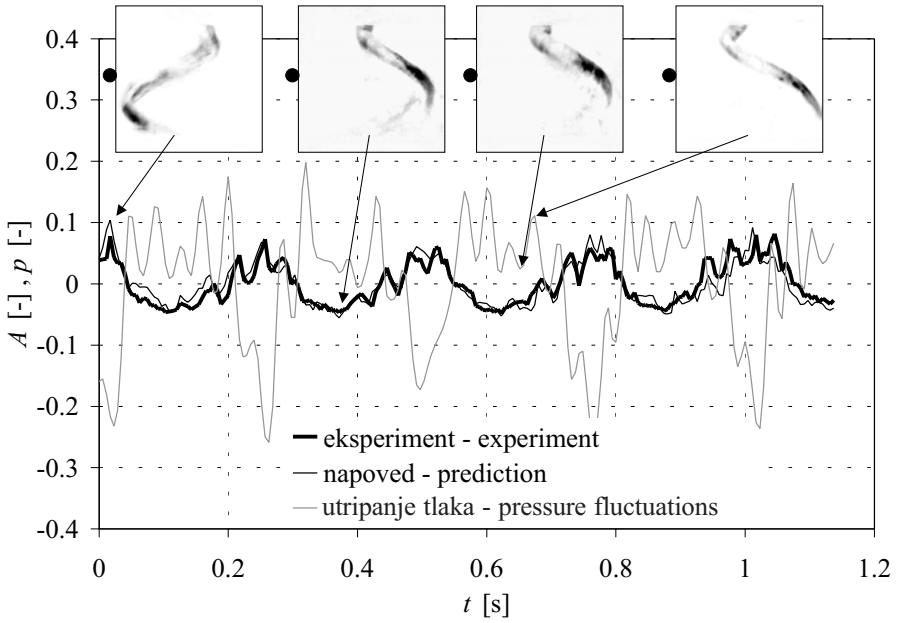

Sl. 6. *Napoved povprečne svetlosti slike, delovna točka 6 (r_w = 0,88). Lega tlačnega zaznavala je prikazana s točko ob posamezni sliki kavitacijskega vrtinca.*
Fig. 6. *Prediction of the average window-intensity operation point 6 (r_w = 0.88). The location of the pressure sensor is shown by a dot beside each representative image.*

Podobni rezultati napovedi kakor v delovni točki 6 so bili doseženi v delovni točki 8 (sl. 7, r_w = 0,82). V tej delovni točki kavitacijski vrtinec kaže nestabilno obnašanje (sl. 10, levo). Opazna so utripanja povprečne svetlosti slike z višjo frekvenco od osnovne, kar je povezano z utripanji tlaka. Napovedana povprečna svetlost slike se dobro ujema z izmerjeno, še posebej pri nizkih, manj pa pri visokih vrednostih povprečne svetlosti slike. Zaradi nestabilne narave tlaka v tej delovni točki tudi večja učna množica ne bi mogla izboljšati kakovosti napovedi. Velika učna množica bi prav tako zahtevala zelo dolg čas za učenje. Zaradi istega razloga nestabilne narave kavitacijskega vrtinca ni mogoče napovedati z metodami, ki temeljijo na parametričnem postopku.

Dobri rezultati, ki so prikazani na slikah 5 do 7, potrjujejo pravilno izbiro metode napovedi. Ugotovili smo, da je mogoče povprečno svetlost slike kavitacijskega vrtinca eksperimentalno napovedati, če poznamo vrednosti tlaka v izbrani točki na steni sesalne cevi. Tehnika bo lahko uporabna za ocenjevanje deleža plinske faze, če predpostavimo, da je povprečna svetlost slike sorazmerna deležu plinske faze v delu, kjer sliko povprečimo. Pri tem bo treba določiti povezavo med povprečno svetlostjo slike in deležem plinske faze.

3.2 Napoved celotnih slik

Pri napovedi celotnih slik določamo strukturo kavitacijskega vrtinca. S primerjavo izmerjenih in napovedanih slik lahko ugotovimo,

A similar prediction performance to operation point 6 was exhibited for operation point 8, shown in Fig. 7 (r_w = 0.82). Here, the vortex exhibits unstable behavior (Fig. 10, left). Fluctuations in the average image intensity with higher frequency than the basic frequency are present, which are related to the pressure fluctuations. The average image intensity follows the measured intensity very well, especially at low values of the average image intensity, and less at high values of the average image intensity. Because of the unstable nature of the pressure at this operation point, even a very large learning set could not improve the prediction performance. A very large learning set would also require a very long time for the learning. For the same reason, the unstable behavior of the cavitation vortex also can not be predicted using other methods, which are based on a parametric approach.

The promising results shown in Figs. 5 to 7 confirm the correct choice of prediction method. We have shown that the average image intensity of the cavitation vortex in the draft tube can be experimentally predicted using the provided pressure measurement for the selected point of the draft-tube wall. The technique could be used for an estimation of the void fraction, assuming that the average image intensity is proportional to the void-fraction volume in the region of the image where averaging is performed. However, the relation between the void fraction and the average image intensity should be established.

3.2 Entire image prediction

By predicting of entire images, the structure of the cavitation vortex is established. By comparing the measured and the predicted images one can

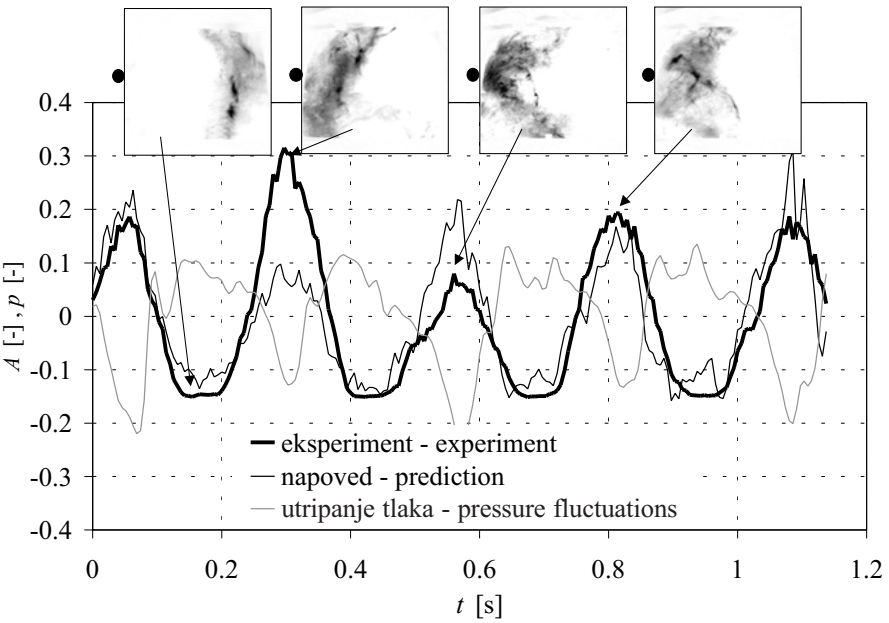

Sl. 7. *Napoved povprečne svetlosti slike, delovna točka 8 (r_w = 0,82). Lega tlačnega zaznavala je prikazana s točko ob posamezni sliki kavitacijskega vrtinca.*

Fig. 7. *Prediction of average window-intensity operation point 8 (r_w = 0.82). The location of the pressure sensor is shown by a dot beside each representative image.*

če časovno zakasnjeni vhodni vektor **x** tlačnih utripanj na steni sesalne cevi vsebuje dovolj informacij za pravilno napoved celotnih slik kavitacijskega vrtinca. Model naj bi določil pravilno strukturo kavitacijskega vrtinca vključno z motnjami na lokalni skali.

Kakor v zgornjem delu bomo preučili napoved celotnih slik v delovnih točkah 12, 6 in 8. Na slikah 8, 9 in 10 so prikazane zaporedne slike kavitacijskega vrtinca, vsako zaporedje pa pomeni eno osnovno periodo gibanja. Levo zaporedje sestavljajo izmerjene slike, desno pa napovedane slike. Zaporedje teče z leve na desno in od zgoraj navzdol.

Svetlost točk na sliki je odvisna poleg strukture kavitacijskega vrtinca tudi od uporabljene osvetlitve. Vpliv osvetlitve zaradi odbojev in senc se pojavlja periodično in je odvisen od strukture vrtinca in njegove lege v sesalni cevi, zato lahko predpostavimo, da ne poslabša kakovosti napovedi.

Rezultati napovedi v delovni točki 12 so prikazani na sliki 8 ($\overline{r}_i$ = 0,88). V tej delovni točki je vrtinec razmeroma debel in stabilen. Rezultati kažejo, da je struktura kavitacijskega vrtinca napovedana pravilno, vključujoč nekatere lokalne podrobnosti.

Slika 9 prikazuje strukturo kavitacijskega vrtinca v delovni točki 6 ($\overline{r}_i$ = 0,62). Kavitacijski vrtinec ima navidezperiodičen značaj. Prostornina kavitacijskega vrtinca se spreminja, to je vrtinec utripa od tanjšega k debelejšemu in nasprotno. To spremljajo utripanja tlačnega signala, prikazuje pa slika 6. Ta utripanja so glavni razlog slabše napovedi

determine whether the time-delayed input vector **x** of the pressure pulsations in the draft-tube wall contains enough information for an appropriate prediction of the entire images of the cavitation vortex. The model should determine the structure of the cavitation vortex, including perturbations on a local scale.

Again, the performance of the entire-image prediction for operation points 12, 6 and 8 will be discussed in more detail. In Figs. 8, 9 and 10, sequences of successive images of the cavitation vortex are shown, each corresponding to one period of motion. The left sections consist of the measured images, while the right sections consist of the corresponding predicted images. The sequence runs from left to right and from top to bottom.

The intensity of the image pixels of the cavitation vortex depends on its structure and on the applied illumination. Influences arising from illumination due to reflections and shadows appear regularly and depend on the vortex structure and the position in the draft tube. It is therefore our assumption that they do not deteriorate the prediction performance.

The results of the prediction of operation point 12 are shown in Fig. 8 ($\overline{r}_i$ = 0.88). Here, the vortex is relatively thick and stable. The results show that the structure of the cavitation vortex is predicted fairly well, including some local details.

Fig. 9 shows the structure of the cavitation vortex for operation point 6 ($\overline{r}_i$ = 0.62). The vortex has a quasi-periodic character. The volume of the cavitation vortex fluctuates, i.e. the vortex changes from thinner to thicker, and vice versa. This is accompanied by fluctuations in the pressure signal, shown in Fig. 6. These fluctuations are the main

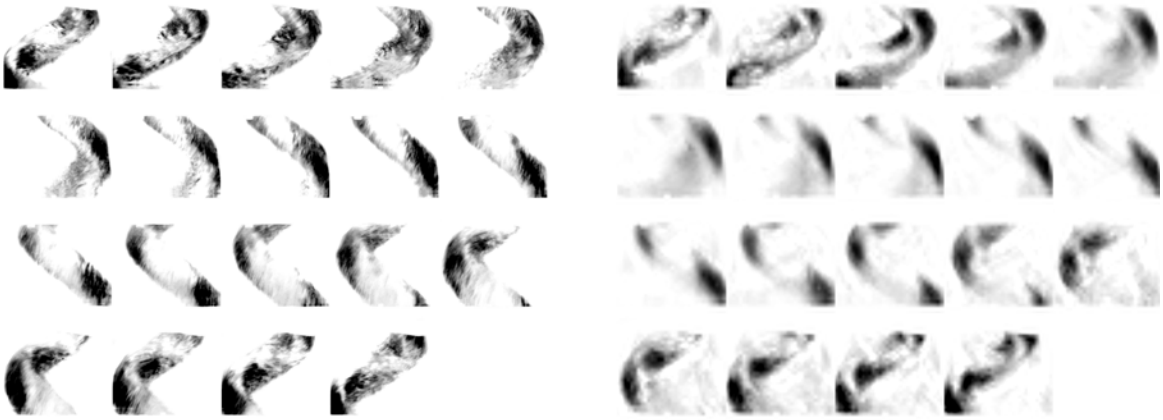

Sl. 8. *Napoved slik kavitacijskega vrtinca, delovna točka 12 ($\overline{r}_i$ = 0,88). Levo : izmerjene slike, desno : napovedane slike. Časovna razlika med zaporednimi slikami je dt = 2/175 s. Zaporedje teče z leve na desno in od zgoraj navzdol ter pomeni eno osnovno periodo gibanja kavitacijskega vrtinca (približno 0,2 s).*

Fig. 8. *Prediction of the cavitation-vortex images, operation point 12 ($\overline{r}_i$ =0.88). Left: measured images, right: predicted images. The time difference between the successive images is dt = 2/175 s. The sequence runs from left to right and from top to bottom, and presents one period of the cavitation-vortex motion (approximately 0.2 s).*

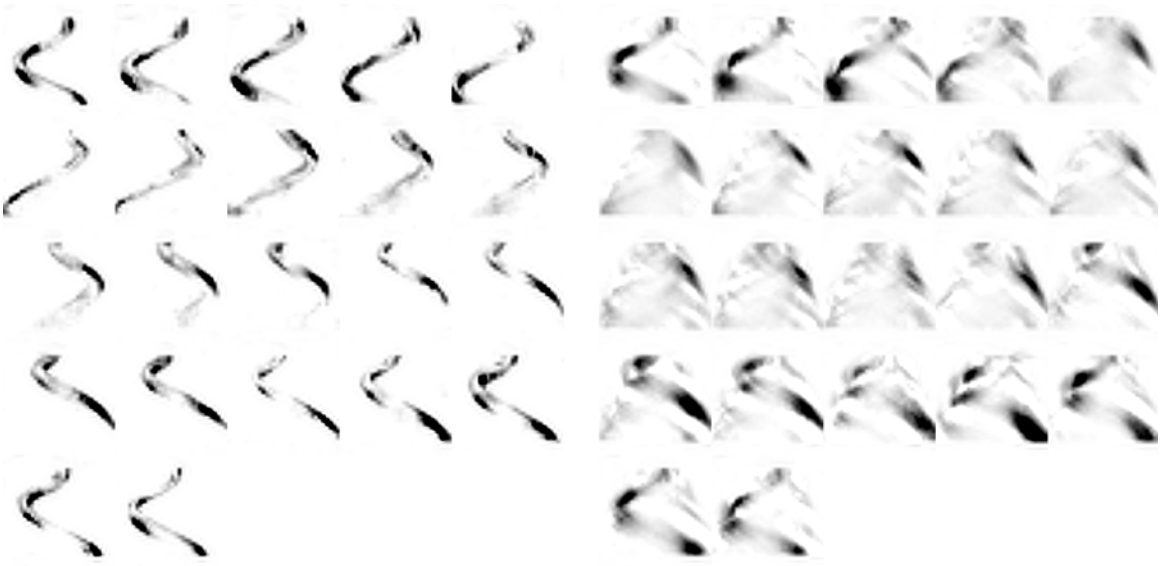

Sl. 9. *Napoved slik kavitacijskega vrtinca, delovna točka 6 ($\overline{r}_i$ = 0,62). Levo : izmerjene slike, desno : napovedane slike. Časovna razlika med zaporednimi slikami je dt = 2/175 s. Zaporedje teče z leve na desno in od zgoraj navzdol ter pomeni eno osnovno periodo gibanja kavitacijskega vrtinca (približno 0,24 s).*

Fig. 9. *Prediction of the cavitation-vortex images, operation point 6 ($\overline{r}_i$ = 0.62). Left: measured images, right: predicted images. The time difference between the successive images is dt = 2/175 s. The sequence runs from left to right and from top to bottom and presents one period of the cavitation-vortex motion (approximately 0.24 s).*

strukture kavitacijskega vrtinca v primerjavi z delovno točko 12 (sl. 8).

Na sliki 10 (delovna točka 8, $\overline{r}_i$ = 0,61) vrtinec kaže težnjo po prehodu iz nestabilnega obnašanja turbulentnega gibanja v organiziran vzorec in nasprotno. Struktura kavitacijskega vrtinca je nestabilna, zaradi česar je kakovost napovedi značilno manjša. To je prikazano na sliki 10 v tretji vrstici.

S slik 8 do 10 lahko ugotovimo, da so bili doseženi boljši rezultati napovedi, ko je bil kavitacijski vrtinec na desni strani slike, gledano z mesta kamere. To ustreza mestu namestitve tlačnega zaznavala, ki je bil prav tako nameščen na levi strani sesalne cevi. Boljše zaznavanje tlačnih utripanj, ki jih povzroča kavitacijski vrtinec, je bilo tako doseženo, ko je bil kavitacijski vrtinec blizu tlačnega zaznavala.

Rezultati potrjujejo, da časovno zakasnjeni vektor **x** tlačnih utripanj vsebuje dovolj informacij za napoved celotnih slik kavitacijskega vrtinca. Metoda se je izkazala kot primerna za razumevanje in krmiljenje pojava. Kljub temu bo v prihodnosti potrebno opraviti še mnogo dela na področju osvetljevanja, predobdelave slik in parametrov nevronskih mrež.

4 SKLEPI

V prispevku je predstavljena simultana študija kinematike kavitacijskega vrtinca in tlačnih

source of the worse prediction of the vortex structure, when compared to operation point 12 (Fig. 8).

In Fig. 10 (operation point 8, $\overline{r}_i$ = 0.61) the vortex shows a tendency to make a spontaneous transition from the unstable behavior of turbulent motion to an organized pattern of motion, and vice versa. The vortex structure has proven to be highly unstable and the prediction performance is significantly lower. This is shown in Fig. 10, third row.

From Figs. 8 to 10 we can see that better prediction results were achieved where the vortex was on the left-hand side of the image, as seen from the camera position. This corresponds to the mounting of the pressure sensor, which was also mounted on the left-hand side of the draft tube. Better sensing of the pressure fluctuations from the vortex was thus achieved when the vortex was close to the pressure sensor.

The presented results confirm that the time-delayed input vector **x** of the pressure pulsations in the draft-tube wall contains enough information for a prediction of entire images of the cavitation vortex. The method has proved to be promissing for understanding and controlling of the phenomenon. However, additional effort should be made in the fields of illumination, image pre-processing and prediction.

4 CONCLUSIONS

A simultaneous study of the kinematics of the cavitation-vortex core in the draft tube of a Francis turbine

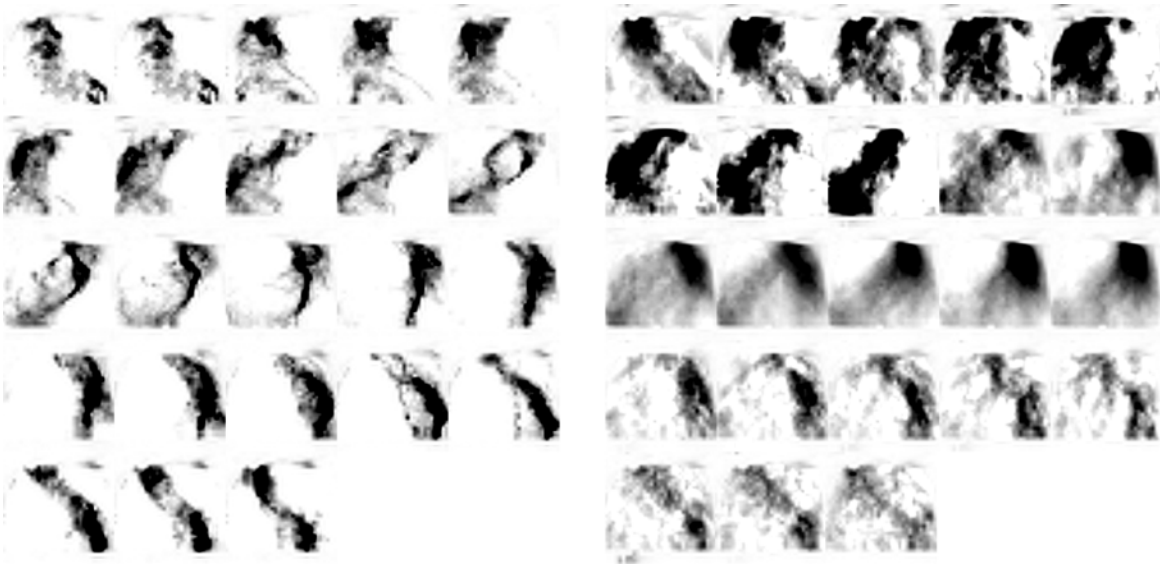

Sl. 10. *Napoved slik kavitacijskega vrtinca, delovna točka 6 ($\overline{r}_i$ = 0,61). Levo : izmerjene slike, desno : napovedane slike. Časovna razlika med zaporednimi slikami je dt = 2/175 s. Zaporedje teče z leve na desno in od zgoraj navzdol ter pomeni eno osnovno periodo gibanja kavitacijskega vrtinca (približno 0,25 s).*

Fig. 10. *Prediction of the cavitation-vortex images, operation point 8 ($\overline{r}_i$ =0.61). Left: measured images, right: predicted images. The time difference between the successive images is dt = 2/175 s. The sequence runs from left to right and from top to bottom and presents one period of the cavitation-vortex motion (approximately 0.25 s).*

utripanj v sesalni cevi francisove turbine. Preučili smo podobnost med izbranimi spremenljivkami in njihovo odvisnost od parametrov pojava. Rezultati potrjujejo, da časovno zakasnjeni vektor tlačnih utripanj na steni sesalne cevi vsebuje dovolj informacij za napoved povprečne svetlosti slik kavitacijskega vrtinca in strukture kavitacijskega vrtinca z uporabo radialnih baznih nevronskih mrež. Rezultati napovedi so bili v povprečju zelo dobri in se ujemajo s predhodno objavljenimi rezultati. Napoved celotnih slik kavitacijskega vrtinca je bila dobra, čeprav je bilo v točkah, v katerih je kavitacijski vrtinec nestabilen, ujemanje slabše.

V prihodnosti se kot možna uporaba kaže študija kavitacijskega vrtinca z naučeno nevronsko mrežo na podlagi umetnega vhodnega signala, kar omogoča modeliranje kinematike vrtinca v sesalni cevi in oblikovanje modelov nadzora toka v sesalnih ceveh.

Kljub dobrim rezultatom, ki so bili predstavljeni zgoraj, nekatere pomanjkljivosti tega in podobnih modelov ostajajo. Med njimi je ostalo pomanjkanje razumevanja o obnašanju kavitacijskega vrtinca v kolenu sesalne cevi. Nadaljnje delo bo potrebno za boljše razumevanje in doseganje končnega cilja, ki je krmiljenje pojava.

and the corresponding pressure pulsations was performed. The results of the study confirm the interdependence of the structural fluctuations of the vortex core and the pressure fluctuations in the draft tube. A similarity between the compared variables and their dependence on the performance parameters of the process was observed. The results of the study confirm that the time-delayed vector of pressure pulsations in the draft-tube wall carries enough information for a prediction of the average image intensity and the structure of the cavitation vortex using radial basis neural networks. The prediction performance was, on average, very good and corresponded well to the previously published results. The entire cavitation-vortex image-prediction performance was good, although in some operation points, where the vortex was unstable, the prediction performance was lower.

As a possible future study, we see the prediction of the cavitation-vortex structure using a trained network by supplying an artificial input signal for the modeling of the cavitation vortex behavior and the development of flow-control models.

In spite of the encouraging results presented above, some of the weaknesses of this and similar models remain. Among them is the lack of an interpretation of the cavitation-vortex behavior in the elbow downstream of the draft tube. Further work will thus be necessary to understand the phenomena and achieve the ultimative aim, which is to control the phenomena.

5 SIMBOLI
5 SYMBOLS

povprečna svetlost slike	A	average image intensity
svetlost točke na sliki	E	pixel intensity
funkcija	f	function
frekvenca tlaka	f_p	pressure frequency
Gaussova funkcija	g	Gaussian function
dolžina časovno zakasnjenega vhodnega vektorja	j	length of time-delayed input vector
število nevronov	K	number of neurons
koordinata točke	l	pixel coordinate
koordinata točke, uteži nevronov	m	pixel coordinate, weights of neurons
število eksperimentalnih vzorcev	N	number of experimental samples
tlačni signal	p	pressure signal
središče sprejemnega polja nevronov	$\mathbf{q}$	center of receptive field of neurons
regresijski koeficient povprečne svetlosti slike	r_w	average image-regression coefficient
regresijski koeficient slike	r_i	entire image-regression coefficient
povprečni regresijski koeficient slike	$\overline{r_i}$	average entire-image regression coefficient
čas	t	time
vhod, časovno zakasnjen tlačni vektor	$\mathbf{x}$	input, time-delayed pressure-pulsations vector
izhod	$\mathbf{y}$	output
širina sprejemnega polja nevronov	s	width of receptive field of neurons
nevronska mreža	NM/ANN	artificial neural network
osrednja procesorska enota	CPE/CPU	central processing unit
diskretna valčna transformacija	DVT/DWT	discrete wavelet transformation
radialna bazna nevronska mreža	RBNM/RBNN	radial basis neural networks

6 LITERATURA
6 REFERENCES

[1] Fanelli, M. (1996) Some present trends in hydraulic machinery research, Proceedings of the XVIII IAHR Symposium on Hydraulic Machinery and Cavitation held in Valencia, Vol.1, *Kluwer Academic Publishers*, Dordrecht.

[2] Fanelli, M. (1999) The cavitated »Vortex Rope« in the draft tube of Francis turbines operating at partial load: a transition from turbulent »chaos« to order?, *9th International Meeting of the IAHR Work Group on the Behaviour of Hydraulic Machinery under Steady Oscillatory Conditions*, Brno.

[3] Brekke, H. (1999) A review on dynamic problems in Francis turbines, *9th International Meeting of the IAHR Work Group on the Behaviour of Hydraulic Machinery under Steady Oscillatory Conditions*, Brno.

[4] Blommaert, G., J.-E. Prenat, F. Avellan, A. Boyer (1999) Active control of Francis turbine operation stability, *Proceedings of the 3rd ASME/JSME Joint Fluid Engineering Conference*, San Francisco.

[5] Qinghua, S. (1994) Estimation of draft tube pressure pulsations for Francis turbines operating at part load conditions, *Proceedings of the XVII IAHR Symposium*, Section on Hydraulic Machinery and Cavitation, Vol.1, Beijing.

[6] Pedrizzetti, G. (1995) A three-dimensional computational approach to the vortex rope dynamics in Francis turbine outlet, *7th International Meeting of the IAHR Work Group on the Behaviour of Hydraulic Machinery under Steady Oscillatory Conditions*, Ljubljana.

[7] Uchiyama, T. (1998) Numerical simulation of cavitating flow using the upstream finite element method, *Applied Mathematical Modelling*, 22, 235-250.

[8] Wang, X., M. Nishi, H. Tsukamoto (1994) A simple model for predicting the draft tube surge, *Proceedings of the XVII IAHR Symposium*, Section on Hydraulic Machinery and Cavitation, Vol.1, Beijing.

[9] Grabec, I., W. Sachse (1997) Synergetics of measurement, prediction and control, *Springer-Verlag*, Berlin.

[10] Gad-el-Hak, M., A. Pollard, and J.-P. Bonnet (1998) Flow control: fundamentals and practices, *Springer-Verlag*, Berlin.

[11] Širok, B., B. Blagojević, T. Bajcar, F. Trenc, *Journal of Hydraulic Research*, in press.

[12] Novak, M., B. Širok, M. Hočevar (1999) Computer vision system as a tool for the analysis of turbulent mixing flows, *9th International Meeting of the IAHR Work Group on the Behaviour of Hydraulic*

Machinery under Steady Oscillatory Conditions, Brno.
[13] Slavič, J., I. Simonovski, M. Boltežar (2002) Uporaba valčne transformacije pri identifikaciji dušenja nihajočih sistemov z več prostostnimi stopnjami, *Zbornik del Kuhljevi dnevi*, Ribno pri Bledu.
[14] Rabbani, M., R. Joshi (2002) An overview of the JPEG 2000 still image compression standard, *Signal Processing: Image Communication*, 17, 3–48.
[15] Mandala, M.K., F. Idrisa, S. Panchanathana (1999) A critical evaluation of image and video indexing techniques in the compressed domain, *Image and Vision Computing*, 17, 513–529.
[16] Markus, H., A. Gross, L.B. Lippert, O.G. Staadt (1999) Compression methods for visualization, Future Generation Computer Systems, 15, 11–29.

Naslov avtorjev: mag. Marko Hočevar
doc.dr. Brane Širok
akad.prof.dr. Igor Grabec
Fakulteta za strojništvo
Univerza v Ljubljani
Aškerčeva 6
1000 Ljubljana
marko.hocevar@fs.uni-lj.si
brane.sirok@fs.uni-lj.si
igor.grabec@fs.uni-lj.si

dr. Tomaž Rus
Turboinštitut
Roušnikova 7
1210 Ljubljana - Šentvid
tomaz.rus@turboinstitut.si

Authors' Addresses: Mag. Marko Hočevar
Doc.Dr. Brane Širok
Akad.Prof.Dr. Igor Grabec
Faculty of Mechanical Eng.
University of Ljubljana
Aškerčeva 6
1000 Ljubljana, Slovenia
marko.hocevar@fs.uni-lj.si
brane.sirok@fs.uni-lj.si
igor.grabec@fs.uni-lj.si

Dr. Tomaž Rus
Turboinstitute
Roušnikova 7
1210 Ljubljana - Šentvid, Slo.
tomaz.rus@turboinstitut.si

Prejeto: 24.7.2003
Received:
Sprejeto: 18.12.2003
Accepted:
Odprto za diskusijo: 1 leto
Open for discussion: 1 year